Thermochimica Acta 555 (2013) 37–45

Contents lists available at SciVerse ScienceDirect

Thermochimica Acta

journal homepage: www.elsevier.com/locate/tca

The crystallization kinetics of Nylon 6/6T and Nylon 66/6T copolymers

Syang-Peng Rwei*, Yu-Chi Tseng, Kuei-Chen Chiu, Shu-Mei Chang, Yu-Ming Chen

Institute of Organic and Polymeric Materials, National Taipei University of Technology, #1, Sec 3, Chung-Hsiao E. Rd., Taipei, Taiwan, ROC

ARTICLE INFO

Article history:
Received 14 August 2012
Received in revised form
26 December 2012
Accepted 30 December 2012
Available online 10 January 2013

Keywords:
Nylon 6/6T
Nylon 66/6T
Crystallization rate
Equilibrium melting point
Isomorphous

ABSTRACT

This work incorporated hexamethylene diamine and terephthalic acid, namely 6T, into typical polymerization processes of Nylon 6 and Nylon 66 to form Nylon 6/6T and Nylon 66/6T copolymers, respectively. The WAXD results showed that as the amount of 6T increased to 10 mol%, all of the Nylon 6/6T copolymers transferred from α-form to γ-form. The DSC measurement revealed that the equilibrium melting point of Nylon 6/6T decreased as the amount of 6T increased. Moreover, the crystallization rate *k* decreased with the 6T content in Nylon 6/6T copolymers, and dropped greatly when the addition of 6T increased over 7 mol%. In contrast, due to the similar molecular chain lengths of Nylon 66 and 6T, the WAXD results of Nylon 66/6T exhibited little crystal difference as the addition of 6T varied from 0 to 30 mol%. The equilibrium melting point of Nylon 66/6T remained constant, proving that Nylon 66/6T is isomorphous.

1. Introduction

Nylon, with its superior strength and heat resistance, is used in automobile industries, electricity-related areas, and electronics. Among the different types of nylons, Nylon 6 and Nylon 66 are the most representative and most common. Nylon 6T, a condensation-type polymer containing hexamethylene diamine and terephthalic acid, is a good engineering plastic with low moisture absorbing capability and good thermal durability. However, due to its high melting point, it is difficult to manufacture. Many commercial products therefore use copolymer to reduce their melting points [1]. Consequently, investigations involving the physical properties of Nylon/Nylon 6T/Additives compounds have been very popular. Due to the close relationship between a material's morphology and its mechanical and thermal properties, research on the crystallization behavior of nylon and its associated materials is very important. Sakurai et al. [2] researched the crystallization of Nylon 6/PAE block copolymer and concluded that dilution decreased the amount of crystals formed by the pure material. This, in turn, decreases the melting point of the copolymer. Lingyu et al. [3] studied the crystallization of Nylon 66/multi-walled carbon nanotube (Nylon 66/MWNT) nanocomposites. According to the estimation by the Avrami method, the *k* value initially increases and then decreases as the MWNT increases. While small quantities of MWNT can form a nucleus to increase the rate of crystallization, excessive MWNT can cause spherulites to interrupt each other, resulting in decreased crystallization speed. Stein and Schreiber et al. [4] achieved double melt peaks of Nylon 66 crystals under different crystallization temperatures, and concluded that melt recrystallization was the cause. The morphology of Nylon 6/montmorillonite nanocomposites was studied by Derek M. [5], indicating the pure nylon 6, 2 wt%, and 5 wt% of Nylon 6/montmorillonite nanocomposites were observed α-form, both α- and γ-form, and increasing α-form with decreasing γ-form, respectively by WAXD in room temperature.

Since terephthalic acid (TPA) replaces adipic acid (AA) in Nylon 66/6T copolymer, and since the chain lengths of AA and TPA are similar, the resulting crystals have high compatibility. Consequently, morphology changes are also relatively minor. This phenomenon is known as isomorphism. This study focuses on the comparison of the crystallization kinetics of isomorphous nylon copolymer (Nylon 66/6T) and nonisomorphous nylon copolymer (Nylon 6/6T). Although some studies have examined the crystallization thermodynamics of Nylon 66/6T copolymer [4,6–8], few of these studies involve the crystallization kinetics of Nylon 6/6T and Nylon 66/6T, which motivates this study.

2. Experimental

In the Nylon 6/6T copolymer used in this experiment, the Nylon 6T ratios were 0 mol%, 3 mol%, 5 mol%, 7 mol% and 10 mol%. For Nylon 66/6T copolymer experiments, the amount of Nylon 6T were 0 mol%, 5 mol%, 10 mol%, 15 mol%, 20 mol%, and 30 mol%. The samples were dried in an oven before the experiment. All of the materials were provided by the Taiwan Textile Research Institute

* Corresponding author. Fax: +886 02 27317174.
E-mail address: f10714@ntut.edu.tw (S.-P. Rwei).

0040-6031/$ – see front matter © 2013 Elsevier B.V. All rights reserved.
http://dx.doi.org/10.1016/j.tca.2012.12.026

Nylon 6/6T:

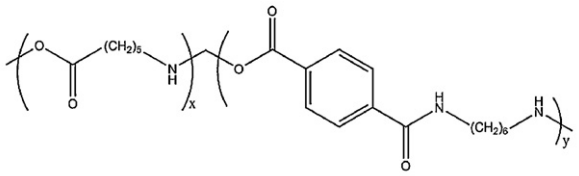

Nylon 66/6T:

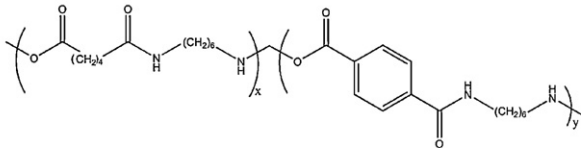

Scheme 1. Chemical structure of Nylon6/6T and Nylon 66/6T copolymers.

(TTRI), which prepared the materials shown below (Scheme 1). Fig. 1(a) and (b) shows typical NMR spectrums of Nylon6/6T and Nylon 66/6T copolymer, respectively. ^{1}H NMR, Bruker Avance DRX400 at 400 MHz, was utilized to identify the chemical structure of the copolymers. Trifluoro acetic acid (TFA) was used as a solvent. The experimental values of 6T % were obtained by the proton peak area of the Nylon 6T divided by those of Nylon 6 (or Nylon 66) plus Nylon 6T (Tables 1a and 1b).

Relative viscosity (RV) was measured using Ubbelohde viscometer, which is a capillary viscometer, operated at a constant temperature 25 °C. The concentration of sample in sulfuric acid (96%) is 1 g/dL. Gel permeation chromatography (GPC) analyses performed herein were on GPC/V2000 of Waters. The well-characterized narrow poly(methyl methacrylate) (PMMA) in hexafluoroisopropanol (HFIP) was used as the calibration standard. Notably, there were no good solvents to dissolve the Nylon 66/6T at high 6T content in the GPC measurement, we therefore mark NA, not available, in Table 1b. However, the consistent RV values indicate that the M_n of Nylon 66/6T in each synthesized case is roughly 40,000 g/mol.

Instruments used for the morphology analysis included X-ray diffractometer (XRD) (PANalytical X'Pert PRO MPD). The XRD sample was first heated to the molten state for 3 min on a hot-stage, and then lowered to a certain temperature at the rate of 120 °C/min for 20 min ($T_c = T_m - 30$ °C). The sample was then placed in liquid nitrogen to preserve the crystal shape. The crystallinity % is calculated by the area of the crystalline peaks divided by total area under the diffraction curve using Topaz Rietveld Refinement software from Bucker.

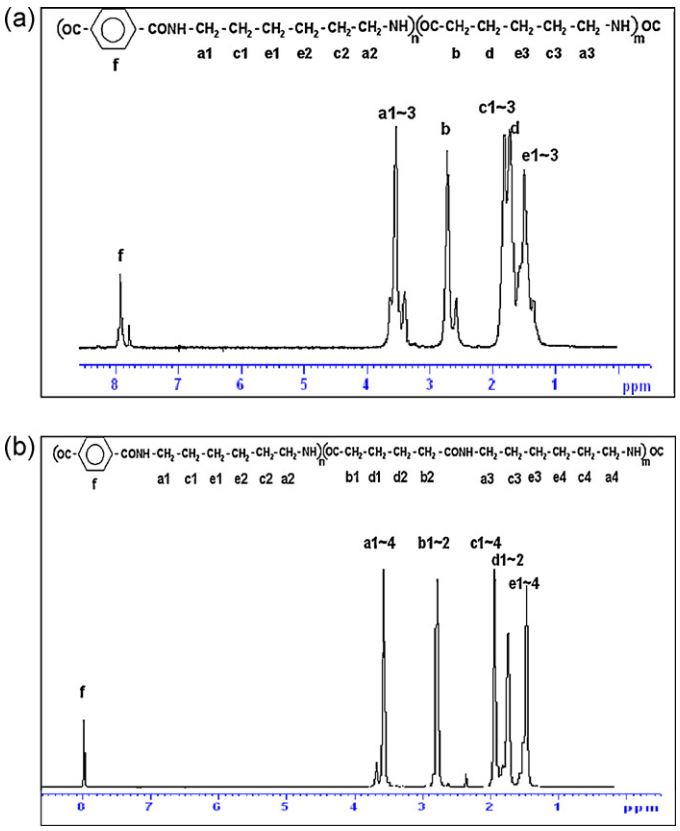

Fig. 1. (a) and (b) H^1 NMR spectrum. (a) Nylon 6/6T 6T 10 mol% copolymer in solvent of TFA, and (b) Nylon 66/6T 6T 10 mol% copolymer in solvent of TFA.

The thermal experiment in this study involved a differential scanning calorimeter (DSC, Perkin-Elmer DSC-7) in a nitrogen-rich environment, increasing the temperature over each sample's

Table 1a
Nylon 6/6T data for ^{1}H NMR, GPC, and RV.

Nylon 6T mol%	0%	3%	5%	7%	10%
^{1}H NMR experimental value	0%	2.36%	4.23%	6.90%	9.79%
M_n (GPC)	29,103	37,944	49,610	42,563	42,868
M_w (GPC)	63,445	74,370	98,228	85,552	85,081
PDI (GPC)	2.18	1.96	1.98	2.01	1.98
RV (relative viscosity)	2.55	2.28	2.36	2.30	2.32

Table 1b
Nylon 66/6T data for 1H NMR, GPC, and RV.

Nylon 6T mol%	0%	5%	10%	15%	20%	30%
^{1}H NMR experimental value	0%	5.74%	10.93%	15.58%	20.77%	28.91%
M_n (GPC)	29,143	39,768	NA	NA	NA	NA
M_w (GPC)	58,869	83,513	NA	NA	NA	NA
PDI (GPC)	2.02	2.10	NA	NA	NA	NA
RV (relative viscosity)	2.51	2.30	2.41	2.31	2.28	2.25

Table 2a
The WAXD results of Nylon6/6T copolymers.

6T	α_1 (°)	L_{200} (nm)	α_2 (°)	$L_{002+202}$ (nm)	Crystallinity (WAXD)	Crystallinity (DSC)
0 mol%	20.20	12.22	23.61	9.56	30.63%	27.24%
3 mol%	20.20	8.55	23.51	8.60	26.25%	24.33%
5 mol%	20.22	8.55	23.54	8.60	17.19%	20.76%

6T	α_1 (°)	L_{001}	Crystallinity (WAXD)	Crystallinity (DSC)
7 mol%	21.15	8.78	16.63%	19.59%
10 mol%	21.06	17.13	11.66%	17.12%

ΔH_f (100%): 240 J/g [18].

Table 2b
The WAXD results of Nylon66/6T copolymers.

6T	α_1 (°)	L_{100}(nm)	α_2 (°)	L_{010} (nm)	Crystallinity (WAXD)	Crystallinity (DSC)
0 mol%	20.26	14.26	23.85	7.17	27.53%	32.36%
5 mol%	20.26	14.26	23.45	8.60	26.25%	31.93%
10 mol%	20.19	14.25	23.45	8.60	27.10%	31.24%
15 mol%	20.23	12.22	23.10	8.60	27.89%	31.82%
20 mol%	20.31	10.69	22.94	7.81	26.36%	31.15%
30 mol%	20.46	8.56	22.74	9.54	25.60%	30.85%

ΔH_f (100%): 196 J/g [4].

melting point at a rate of 20 °C/min. Nylon 6/6T and Nylon 66/6T copolymers were heated to 250 °C and 300 °C, respectively. These temperatures were maintained for 3 min to remove thermal history. An isothermal crystallization experiment was then performed by rapidly cooling the samples at the rate of 200 °C/min to a targeted crystallization temperature, and then by holding the temperature constant for 20 min. After crystallization was completed, the temperature increased at the rate of 20 °C/min until the samples became molten again. The molten peaks were then observed.

A polarized optical microscope (POM, Nikon LABOPHOT2) was performed for Nylon 66, Nylon 66/6T-5%, and Nylon 66/6T-10% samples in this work. The temperatures was first increased to 300 °C, and then rapidly reduced to crystallization range (227.5–240 °C) for observing the crystal formation. The crystal formation rates could thus be obtained by measuring the spherulite

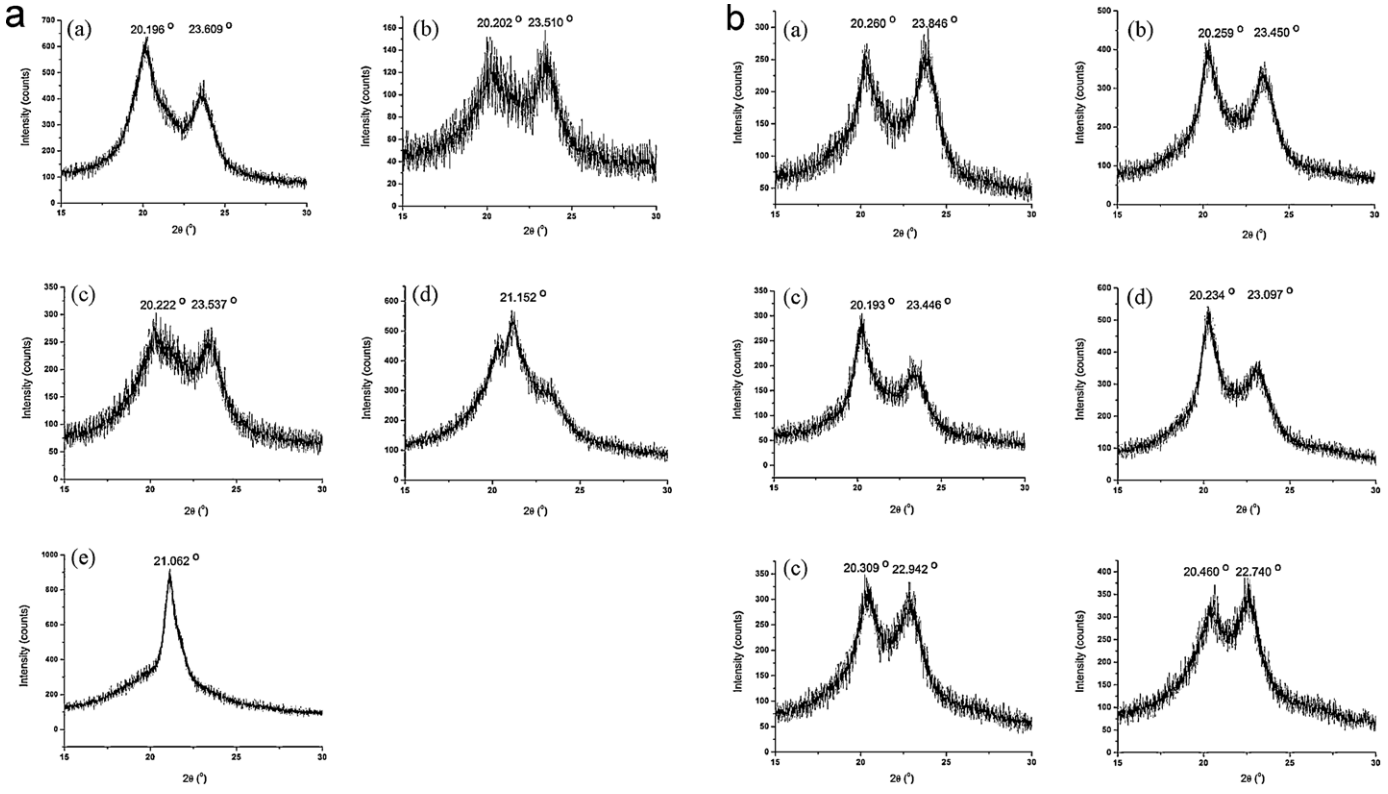

Fig. 2. (a) and (b) The comparison between theoretical and experimental value. (a) The mol% for Nylon 6/6T copolymers. (b) The mol% for Nylon 66/6T copolymers.

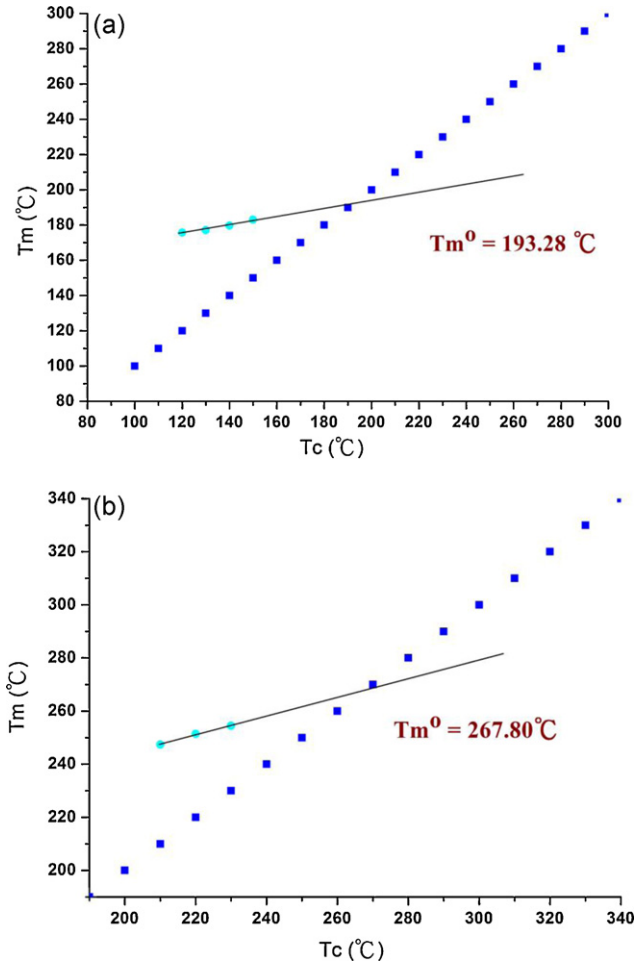

Fig. 3. The plot to determine the equilibrium melting temperature by Hoffman–Weeks method for (a) Nylon 6/6T 7 mol% (b) Nylon 66/6T 20 mol%.

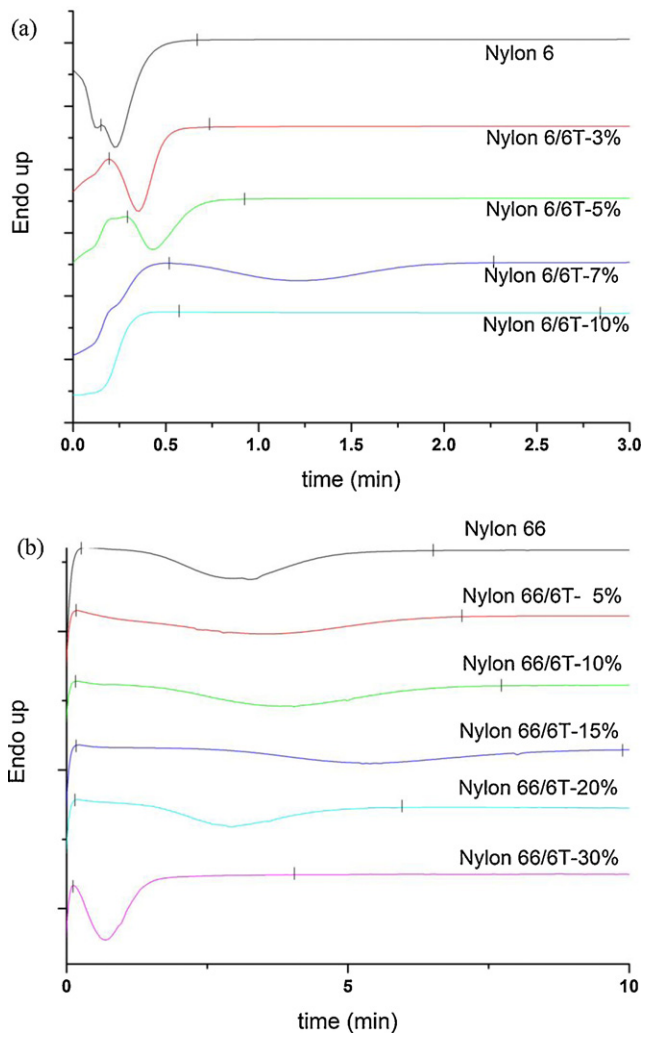

Fig. 4. The isothermal crystallization curves for (a) Nylon 6/6T of different copolymerization ratios at 150 °C (b) Nylon66/6T of different copolymerization ratios at 240 °C. (The starting and ending point of the exothermic peak in the curve are marked.)

size from the photo image at a specific time before the crystals collided with each other.

3. Results and discussion

3.1. Crystallization thermodynamics study

Fig. 2(a) shows the wide-angle X-ray diffraction (WAXD) results of Nylon 6/6T copolymer. This figure demonstrates that pure Nylon 6 exhibited α-form. As the quantity of 6T increased to 7 mol%, both α-form and γ-form appeared [9–11]. When Nylon 6T reached 10 mol%, all of the copolymers presented γ-form. The α-form represents a stable crystal structure in a triclinic type. The γ-form, in contrast, represents an unstable crystal structure in a monoclinic type. The γ-form can convert to the α-form with increased temperature or crystallization time. The existence of a benzene ring of nylon 6T might retard the chain mobility and inhibit this conversion, causing the entire crystal structure to remain in the γ-form [12,13].

Fig. 2(b) shows the WAXD results of Nylon 66/6T copolymers. Compared to Nylon 6/6T copolymers, Nylon 66/6T copolymers exhibit very few differences in the crystal patterns regardless of the variation in copolymerization ratio. The primary reason is that the replacement of adipic acid in nylon 66 with terephthalic acid in nylon 66/6T is a good example of "isomorphism." [14,15] This isomorphous replacement not only indicates that the distance between the functional groups is about the same, but also that the orientation of the comonomer units in the crystal lattice must be identical. The length of four methylene groups of adipic acid is 0.508 nm. Meanwhile, the length of the benzene ring of terephthalic acid to the direction of chain length at an angle of 35° is 0.510 nm. This slight displacement might make the crystal structure of nylon 66 [16,17] the same as nylon 66/6T.

Tables 2a and 2b list the WAXD characteristic peaks of Nylon6/6T and Nylon 66/6T copolymers, respectively. The degree of crystallization for each condition was calculated thereafter. Table 2a shows that as the amount of Nylon 6T increases from 0 to 10 mol% in Nylon 6/6T copolymer, the crystallization degree decreases from 30.63% to 11.66. For Nylon 66/6T copolymers, and the degree of crystallization remained at approximately 26.36% regardless of the copolymerization ratios. Similarly, DSC measurement shows that the crystallization degree of Nylon 6/6T copolymer decreased from 27.24% to 17.12%, while that of Nylon 66/6T copolymer remained stable at approximately 31.15%. Furthermore, the Scherrer equation [18–20] calculated the crystal thickness:

$$L_{hkl} = \frac{k \times \lambda \times 180}{\beta \times \cos\theta \times \pi} \quad (1)$$

where L_{hkl} is the cystal thickness perpendicular to a given planes (hkl), k is the Scherrer shape factor which adopts value close to a

Table 3
The thermal properties of Nylon6/6T and Nylon66/6T copolymers by DSC.

Sample	T_g (°C)	ΔH_f (J/g)	T_m (°C)	T_m^o (°C)
Nylon 6	43	93.8	225	258
Nylon 6/6T-3%	46	79.9	217	235
Nylon 6/6T-5%	47	72.9	202	208
Nylon 6/6T-7%	51	72.0	191	193
Nylon 6/6T-10%	56	66.5	189	191
Nylon 66	44	79.6	265	275
Nylon 66/6T-5%	45	70.6	264	272
Nylon 66/6T-10%	51	69.8	263	268
Nylon 66/6T-15%	52	66.0	262	267
Nylon 66/6T-20%	54	62.4	264	268
Nylon 66/6T-30%	64	58.1	272	277

constant of 0.9, λ is the wavelength of the X-ray (0.5418 nm), and β is the full width at half maximum (FWHM) of the peak. Results shown in Table 1 (L_{200} for Nylon 6/6T) and Table 2 (L_{100} for Nylon 66/6T) indicate that the lamellae thickness in the copolymer was thinner than that of pure polymers, confirming that the presence of Nylon 6T reduced the size of crystal domain.

Table 3 shows that melting point and enthalpy decreased as the amount of Nylon 6T increased. This is because Nylon 6T disrupted the crystal lattice of Nylon 6, causing the degree of crystallization and melting point to decrease. In addition, the addition of Nylon 6T increased the rigidity of the copolymer, which explains why the glass transition point (T_g) increased. Due to the similar chain

Table 4
The parameters of crystallization kinetics of Nylon 6/6T and Nylon 66/6T copolymers calculated using Avrami Equation.

(a)

T_c (°C)	130	140	150	160	170	180
Nylon 6						
n	1.42	1.56	1.62	1.99	2.14	1.87
k (min^{-n})	33.73	34.04	27.79	10.30	4.20	0.98
$t_{1/2}$ (min)	0.065	0.082	0.102	0.258	0.431	0.829
Nylon 6/6T-3%						
n	2.03	2.01	1.96	1.93	1.97	2.74
k (min^{-n})	31.70	29.50	26.16	12.98	2.83	0.32
$t_{1/2}$ (min)	0.152	0.155	0.157	0.219	0.489	1.325
Nylon 6/6T-5%						
n	1.90	1.87	1.83	2.07	2.51	2.93
k (min^{-n})	28.52	26.59	14.49	2.96	0.092	0.002
$t_{1/2}$ (min)	0.141	0.142	0.190	0.496	2.233	7.074
Nylon 6/6T-7%						
n	1.78	2.02	2.56	2.66	2.64	–
k (min^{-n})	4.20	3.41	1.44	0.186	0.022	–
$t_{1/2}$ (min)	0.363	0.455	0.752	1.640	3.682	–
Nylon 6/6T-10%						
n	2.35	2.64	2.61	–	–	–
k (min^{-n})	0.445	0.129	0.009	–	–	–
$t_{1/2}$ (min)	1.207	1.891	5.215	–	–	–

(b)

T_c (°C)	200	210	220	230	240
Nylon 66					
n	2.01	1.93	1.58	2.18	2.71
k (min^{-n})	38.67	20.93	10.89	3.85	0.099
$t_{1/2}$ (min)	0.135	0.171	0.175	0.455	2.049
Nylon 66/6T-5%					
n	1.74	1.58	1.62	1.87	2.41
k (min^{-n})	36.90	21.61	6.60	0.96	0.052
$t_{1/2}$ (min)	0.102	0.114	0.250	0.840	2.926
Nylon 66/6T-10%					
n	1.67	1.67	1.88	2.33	2.67
k (min^{-n})	29.49	17.43	5.78	0.78	0.042
$t_{1/2}$ (min)	0.106	0.146	0.323	0.949	2.870
Nylon 66/6T-15%					
n	1.72	1.65	1.85	2.29	2.50
k (min^{-n})	28.52	14.63	4.81	0.80	0.037
$t_{1/2}$ (min)	0.115	0.158	0.351	0.942	3.179
Nylon 66/6T-20%					
n	1.72	1.56	1.69	2.21	2.21
k (min^{-n})	31.35	22.75	13.42	4.18	0.278
$t_{1/2}$ (min)	0.110	0.107	0.174	0.443	1.512
Nylon 66/6T-30%					
n	1.79	1.61	1.57	1.69	2.08
k (min^{-n})	40.06	21.47	13.52	5.40	1.63
$t_{1/2}$ (min)	0.103	0.118	0.152	0.298	0.662

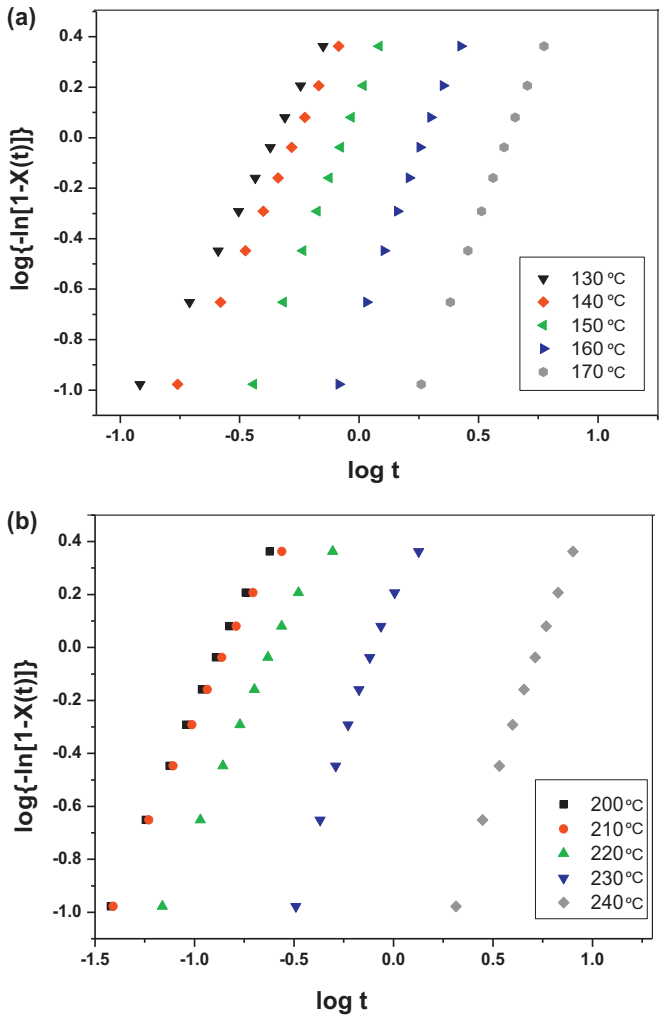

Fig. 5. The retreatment of Fig. 4 by Avrami method for (a) Nylon 6/6T 7 mol% at various crystallization temperatures (b) Nylon 66/6T 20 mol% at various crystallization temperatures.

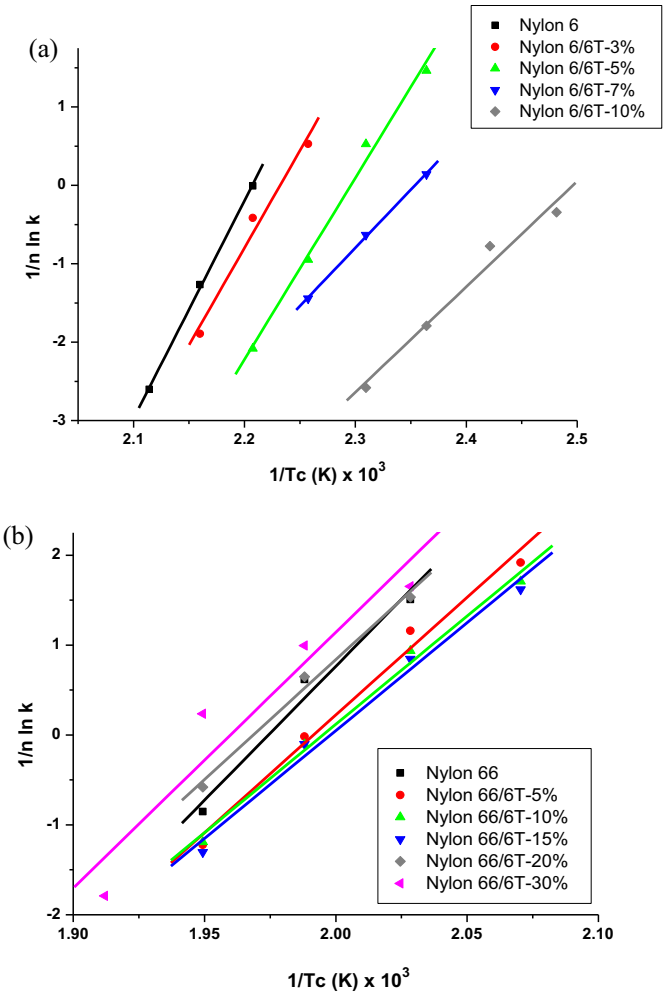

Fig. 6. The retreatment of Table 4 to obtain the crystallization activation energy ΔE_a. of (a) Nylon 6/6T copolymers (b) Nylon 66/6T copolymers.

lengths between Nylon 6T and Nylon 66, Nylon 6T was able to fit into the crystal lattice of Nylon 66 and cause little impact on the melting point. In contrast, T_g increased as Nylon 6T increased. In general, T_g depends heavily on the rotational energy requirements of the polymer backbone. Addition of Nylon 6T to Nylon 6 or Nylon 66 reduces its rotation capability. The T_g of Nylon 66/6T or Nylon 6/6T therefore increases with the mol% of Nylon 6T.

After isothermal melt crystallization, the Hoffman–Weeks equation was used to obtain the equilibrium melting point. This equation is shown as follows [21–24]:

$$T_m = T_m^o\left(1 - \frac{1}{\gamma}\right) + \left(\frac{1}{\gamma}\right)T_c \quad (2)$$

where T_m is the experimentally obtained melting point, γ represents a stability parameter that depends on the crystal size and perfection, and T_m^o is the equilibrium melting point. The T_m^o and γ can therefore be calculated by using two set of T_m and T_c. This experiment revealed double melting peaks, suggesting that melt recrystallization [22] induces the higher melting peak. The lower melting peak was therefore selected as the equilibrium melting point. Fig. 3(a) and (b) shows typical Hoffman–Week plots of Nylon 6/6T and Nylon 66/6T copolymers, respectively, and Table 3 lists the associated results. Experimental results indicate that owing to the dilution of regulated chain length of Nylon 6, the equilibrium melting point T_m^o of Nylon 6/6T copolymer decreased as the amount of Nylon 6T increased. In contrast, due to the similar molecular chain lengths of Nylon 66 and 6T, the T_m^o of Nylon 66/6T remained constant until the amount of Nylon 6T reached 30 mol%. At this point, the melting point increased by 8 °C which is attributed to the attraction force of the benzene rings among 6-T segments.

3.2. Isothermal crystallization kinetics study

Fig. 4(a) and (b) respectively show the DSC spectrums of Nylon 6/6T copolymer at 150 °C and Nylon 66/6T copolymer at 240 °C, displaying the relationship between melt peaks and time. The Avrami equation analyzed the samples in Fig. 4 as follows [25–30]:

$$X(t) = 1 - \exp(-kt^n) \quad (3)$$

The time-dependent volume fraction crystallinity $X(t)$ can be determined by integrating the isothermal DSC curve from t_0 to t, the t_0 defined herein is the instant when the slope of DSC curve becomes zero in the beginning stage, k is the Avrami rate constant, and n is the Avrami exponent or shape parameters, indicating the type of nucleation and shape of crystal growth. Reorganizing the equation leads to the following equation:

$$\log\{-\ln[(1 - X(t)]\} = n\log t + \log k \quad (4)$$

Graphing $\log\{-\ln(1 - X(t)\}$against $\log t$ produces a graph with intercept $\log k$ and slope n. Substituting these values back into the

Table 5
The crystallization activation energy of Nylon6/6T and Nylon66/6T copolymers.

Nylon 6/6T (mol%)	0	3	5	7	10	
E_a (kJ/mol)	−230.94	−206.15	−192.61	−123.40	−111.87	
Nylon 66/6T (mol%)	0	5	10	15	20	30
E_a (kJ/mol)	−247.84	−217.90	−200.28	−199.54	−221.92	−236.60

Avrami equation and setting the time at which crystallization was 50% complete to $t_{1/2}$ produces the following equation:

$$t_{1/2} = \left(\frac{\ln 2}{k}\right)^{1/n} \quad (5)$$

Fig. 5(a) and (b) shows graphs displaying relationship of Nylon 6/6T-7% and Nylon 66/6T-20%, respectively. Table 4 lists the calculation results, showing that at the same crystallization temperature, increasing the presence of Nylon 6T in Nylon 6/6T copolymer to 7 mol%, or further to 10 mol%, k decreased significantly in both cases. This is because the crystal lattices of Nylon 6T and Nylon 6 are incompatible, making crystallization extremely difficult and reducing the overall rate of crystallization. On the other hand, the k values of Nylon 66/6T copolymer at 200 °C were all in the range of 30–40, proving that Nylon 66/6T is an isomorphous copolymer. Table 4 also reveals that the k value of Nylon 66/6T copolymer decreased initially and then increased as the amount of Nylon 6T increased over 15 mol%. The rate constant k increases is influenced by the increase in the number of nuclei resulted from adding a large quantity of 6T. Noticeably, the lowest k value occurred when the amount of Nylon 6T of Nylon 66/6T copolymer was approximately 15 mol%. This implies that although Nylon 66/6T is an isomorphous copolymer, the addition of 15% Nylon 6T would be less compatible and causes a transition state in the morphology evolution. These results indicate that Nylon 66/6T is not perfectly isomorphous at certain ratios.

Polymer crystallization activation energy includes the activation energy of molecular bond movements and that of nucleation. This is usually obtained using the Arrheius equation [31–34] as follows:

$$k^{1/n} = k_0 \exp\left(\frac{-E_a}{RT_c}\right) \quad (6)$$

$$\left(\frac{1}{n}\right)\ln k = \ln k_0 + \left(\frac{-E_a}{R}\right)\left(\frac{1}{T_c}\right) \quad (7)$$

where k is the crystallization rate constant, k_0 is a preset factor (not directly related to temperature), n is the Avrami index, T_c is the temperature of isothermal crystallization (K), E_a is the activation energy required (kJ/mol), and R is the ideal gas constant. Using curve fitting of the Avrami equation for each isothermal condition, n and k values were determined and substituted into Eq. (7). Then graphs of $(1/n)\ln k$ versus $(1/T_c)$ were made in Fig. 6(a) and (b). A slope of $-\Delta E_a/R$ was obtained, which includes the isothermal crystallization activation energies of the samples (Table 5). Table 5 reveals that the crystallization activation energy of Nylon 6/6T copolymer increased as Nylon 6T increased. The activation energies of Nylon 66/6T copolymers were similar to each other, but were still the

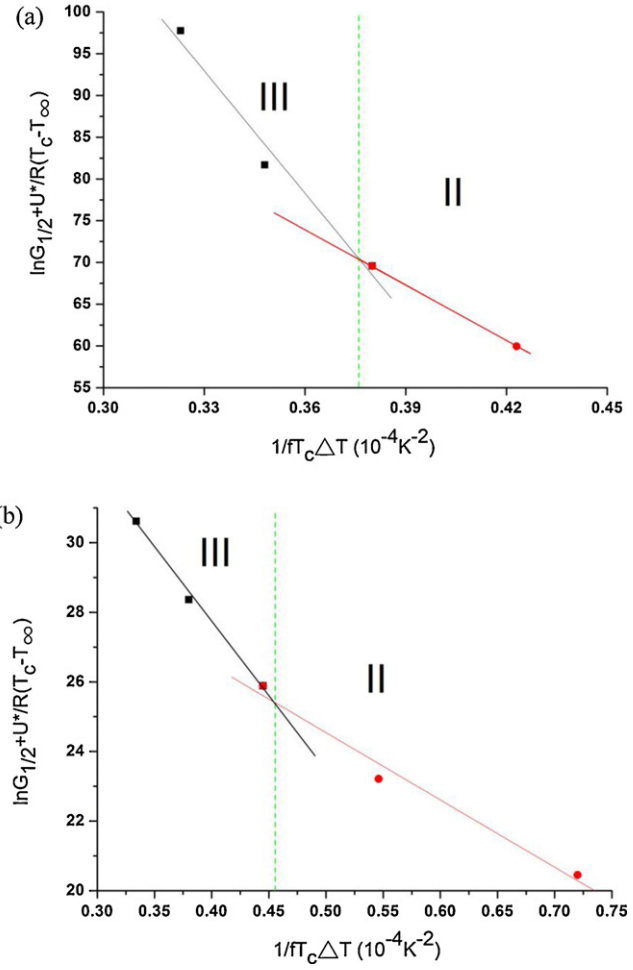

Fig. 7. The plot of nucleation rate against $1/T_c$ following Lauritzen–Hoffman analysis for (a) Nylon 6/6T 7 mol% (b) Nylon 66/6T 20 mol%.

Table 6
The results of nucleation analysis (Stage II to Stage III) using Lauritzen–Hoffman method.

Sample	$Kg_{III} \times 10^{-5}$	$Kg_{II} \times 10^{-5}$	$KgIII/Kg_{II}$	Transition temperature (°C)
Nylon 6	51.75	25.35	2.04	150.1
Nylon 6/6T-3%	48.34	24.40	2.00	138.9
Nylon 6/6T-5%	45.30	20.88	2.17	129.0
Nylon 6/6T-7%	49.41	22.23	2.22	122.8
Nylon 6/6T-10%	42.15	24.14	1.75	120.0
Nylon 66	4.43	2.44	1.82	224.0
Nylon 66/6T-5%	4.78	2.37	2.02	221.5
Nylon 66/6T-10%	4.13	1.90	2.18	221.8
Nylon 66/6T-15%	4.10	1.87	2.20	221.6
Nylon 66/6T-20%	4.24	1.93	2.20	221.9
Nylon 66/6T-30%	5.42	2.49	2.18	228.3

highest when the content of Nylon 6T was approximately 15 mol%. This result is similar to the crystallization rate constant k obtained in the Avrami equation and has an identical explanation.

3.3. Lauritzen–Hoffman analysis

Regime changes during crystallization allow us to identify what mechanism controls the crystallization rate. First, the Lauritzen–Hoffman equation was used to analyze the sample's crystallization rate. This equation is as follows [35–40]:

$$G = G_0 \exp\left(\frac{-U^*}{R \times (T_c - T_\infty)}\right) \exp\left(\frac{-K_g}{T_c \times \Delta T \times f}\right) \quad (8)$$

where G_0 is predetermined value, T_c is the crystallization temperature, R is the gas constant, and U^* is the activation energy needed for molecular chains to move to crystal position in molten state. Using the WLF equation obtains the following equation [41,42]:

$$U* = \frac{C_1 T_c}{C_2 + T_c - T_g} \quad (9)$$

where $C_1 = 17{,}304$ J/mol, $C_2 = 51.6$ K, T_∞ is the temperature at which the molecular chain stops moving (T_∞ (K) = T_g (K) − 30), ΔT is the temperature change $\Delta T = T_m^o - T_c$, f is the correction factor for enthalpy and temperature reliance, and K_g is a nucleation constant. Consequently, graphing $\ln G + U^*/[R(T_c - T_\infty)]$ against $1/(fT_c\Delta T)$ produces a line with slope of $-K_g$ and an intercept of $\ln G_0$. The critical temperature at which Regime II converted to Regime III occurred when the ratio of K_g(III)/K_g(II) equals 2. Region II growth occurred by multiple nucleation and normal spherulites formed in region II. Region III growth occurred by prolific multiple nucleation. Region III indicates rapid cooling. The chains do not undergo repeated adjacent reentry into the lamellae, but have only a few folds before entering the amorphous phase or going on to the next lamella. Fig. 7(a) and (b) shows relevant spectroscopy results of Nylon 6/6T-7% and Nylon 66/6T-20%, as Table 6 presents the data. As the amount of Nylon 6T in Nylon 66/6T copolymers increased, the critical temperature at which Regime II converted to Regime III decreased. On the other hand, the critical conversion temperatures in Nylon 66/6T were close to each other. The benzene ring and lattice in Nylon 6/6T were incompatible, causing the lamellae to be small and defective. This was beneficial to the rate of instantaneous nucleation, increasing the slope of Regime III. Consequently, the conversion temperature from Regime II to III decreased in Nylon 6/6T as the amount of Nylon 6T increased, but remained relatively constant in Nylon 66/6T due to the isomorphous effects.

Fig. 8 shows the isothermal crystallization of Nylon 66 at 230 °C and Fig. 9 graphs the rate of its crystallization. Results indicate that as the crystallization temperature decreased, the rate of crystallization increased. This result matches the DSC crystallization kinetics study discussed before.

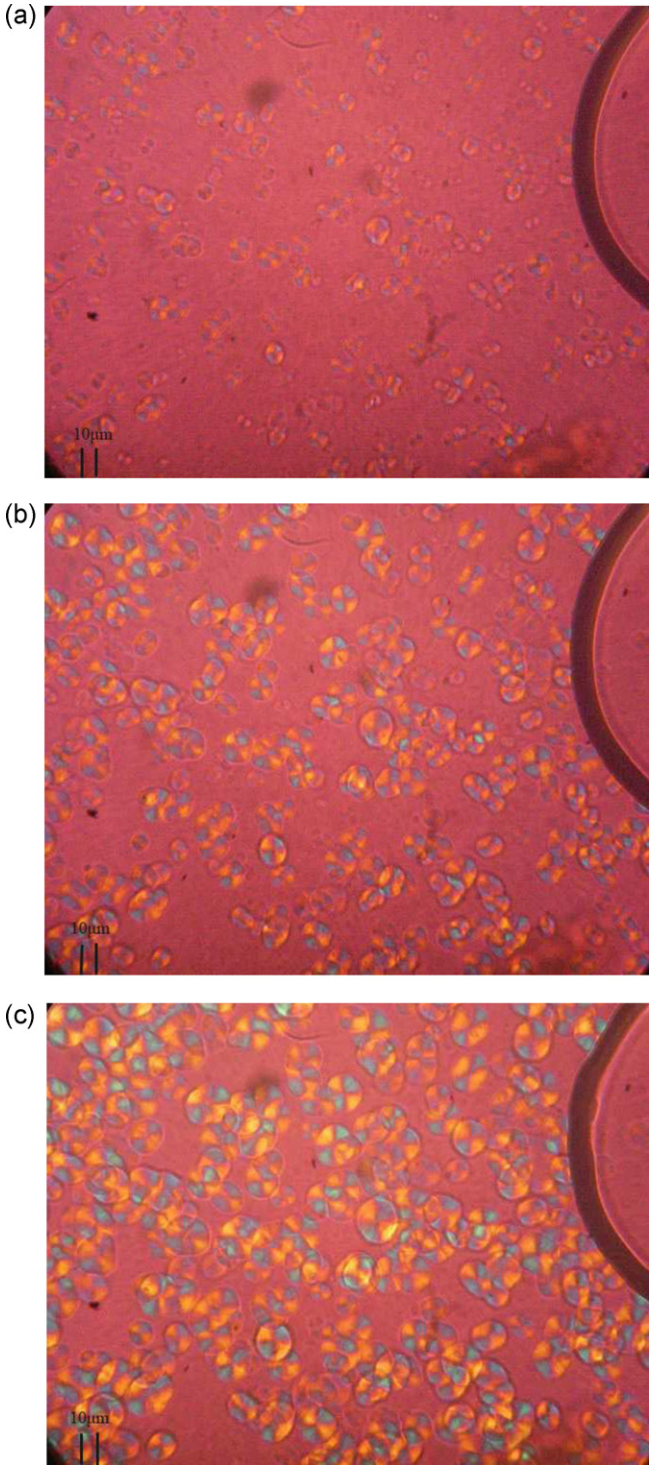

Fig. 8. (a)–(c) The snapshot of spherulite growth process, using polarized optical microscope, for Nylon66/6T 5 mol% at 230 °C on 3, 6, and 9 s, respectively.

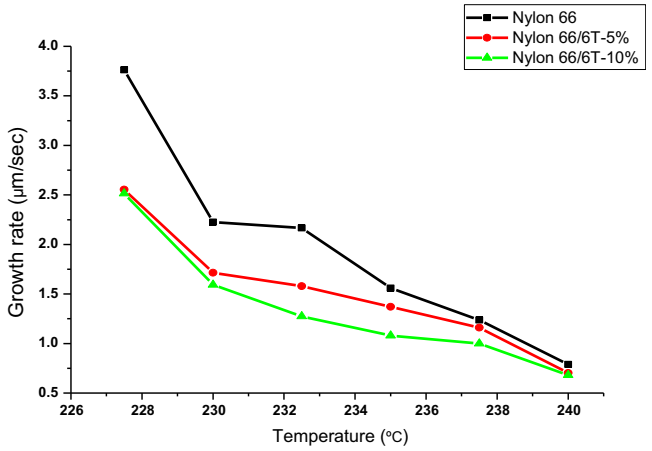

Fig. 9. The dependence of spherulite growth rate on temperature for Nylon 66/6T copolymers.

4. Conclusions

4.1. Crystallization thermodynamics study

The WAXD results demonstrate that pure nylon 6 exhibited α-form. As the amount of 6T increased to 7 mol%, both α-form and γ-form appeared. When Nylon 6T reached 10 mol%, all of the copolymers exhibited the γ-form. However, the WAXD results of Nylon 66/6T copolymers exhibited little difference as the addition of Nylon 6T varied from 0 to 30 mol%. Similarly, the DSC measurement revealed that the equilibrium melting point of Nylon 6/6T copolymer decreased as the amount of Nylon 6T increased. In contrast, due to the similar molecular chain lengths of Nylon 66 and 6T, the equilibrium melting point of Nylon 66/6T remained constant until the amount of Nylon 6T reached 30 mol%.

4.2. Isothermal crystallization kinetics study

The crystallization rate k decreased with the Nylon 6T mol%. Moreover, k dropped greatly as the addition of Nylon 6T increased to 7 mol%. In contrast, the k values of Nylon 66/6T copolymer at 200 °C were all in the range of 30–40, proving that Nylon 66/6T is an isomorphous copolymer. However, the lowest k value occurred when the amount of Nylon 6T in Nylon 66/6T copolymer was approximately 15 mol%. This result indicates that Nylon 66/6T is not perfectly isomorphous at any given ratio.

The crystallization activation energy of Nylon 6/6T copolymer increased as Nylon 6T increased. The activation energies of Nylon 66/6T copolymers were similar to each other, but were still the highest when the content of Nylon 6T was approximately 15 mol%.

As the amount of Nylon 6T in Nylon 66/6T copolymers increased, the critical temperature at which Regime II converted to Regime III decreased. However, the critical conversion temperatures remained relatively constant in Nylon 66/6T due to the isomorphous effect.

References

[1] M.J. Robinson, R.O. Charette, B.G. Leonard, Advanced composite structures for launch vehicles, SAMPE Q. 22 (1991) 26–37.
[2] K. Sakurai, G. Amador, T. Takahashi, Block copolymers based on nylon 6 and poly(propylene glycol). I. Structure and thermal properties, Polymer 39 (1998) 4089–4094.
[3] L. Li, C.Y. Li, C. Ni, L. Rong, B.S. Hsiao, Structure and crystallization behavior of Nylon 66/multi-walled carbon nanotube nanocomposites at low carbon nanotube contents, Polymer 48 (2007) 3452–3460.
[4] S.S. Lee, P.J. Phillips, Melt crystallized polyamide 6.6 and its copolymers, part I. Melting point – lamellar thickness relations in the homopolymer, Eur. Polym. J. 43 (2007) 1933–1951.
[5] D.M. Lincoln, R.A. Vaia, Z.G. Wang, B.S. Hsiao, R. Krishnamoorti, Crystallisation behaviour of polyamide-6 and polyamide-66 nanocomposites, Polymer 42 (2001) 9975–9985.
[6] Q.X. Zhang, Z.S. Mo, Melting crystallization behavior of nylon 66, Chin. J. Polym. Sci. 19 (2001) 237–246.
[7] M.I. Kohan, Nylon Plastics Handbook, Hanser Gardner Publications Inc., New York, 1995 (Chapter 2).
[8] D. Beaton, US Patent (1974) 3,821 171.
[9] T.D. Fornes, D.R. Paul, Crystallization behavior of nylon 6 nanocomposites, Polymer 44 (2003) 3945–3961.
[10] M.I. Kohan, Nylon Plastics Handbook, Hanser Gardner Publications Inc., New York, 1995 (Chapter 5).
[11] Z. Zhao, W. Zheng, H.W. Tian, W. Yu, D. Han, B. Li, Crystallization behaviors of secondarily quenched nylon 6, Mater. Lett. 61 (2007) 925–928.
[12] J.O. Karlsson, M. Andersson, P. Berntsson, T. Chihani, P. Gatenholm, Swelling behavior of stimuli-responsive cellulose fibers, Polymer 39 (1998) 3585–3595.
[13] J. Zheng, R.W. Siegel, C.G. Toney, Polymer crystalline structure and morphology changes in nylon-6/ZnO nanocomposites, J. Polym. Sci. Part B: Polym. Phys. 41 (2003) 1033–1050.
[14] M.I. Kohan, Nylon Plastics Handbook, Hanser Gardner Publications Inc., New York, 1995, pp. 370–374 (Chapter 2).
[15] R.J. Gaymans, S. Aalto, F.H.J. Maurer, Copolyamides of nylon-4,6 and nylon-4,T, J. Polym. Sci. Part A: Polym. Chem. 27 (1989) 423–430.
[16] X. Kang, S. He, C. Zhu, L. Wanhm, L. Lu, J. Guo, Studies on crystallization behaviors and crystal morphology of polyamide 66/clay nanocomposites, J. Appl. Polym. Sci. 95 (2005) 756–763.
[17] R. Brill, Über das Verhalten von Polyamiden beim Erhitzen, J. Prakt. Chem. 161 (1942) 49–64.
[18] L.E. Alexander, X-ray Diffraction Methods in Polymer Science, Wiley, New York, 1969.
[19] X. Zhao, J. Cheng, S. Chen, J. Zhang, X. Wang, Controlled crystallization of poly(vinylidene fluoride) chains from mixed solvents composed of its good solvent and nonsolvent, J. Polym. Sci. Part B: Polym. Phys. 48 (2010) 575–581.
[20] G. Zhao, Y. Men, Z. Wu, X. Ji, W. Jiang, Effect of shear on the crystallization of the poly(ether ether ketone), J. Polym. Sci. Part B: Polym. Phys. 48 (2010) 220–225.
[21] J.D. Hoffman, J.J. Weeks, Regime III crystallization in melt-crystallized polymers: the variable cluster model of chain folding, J. Res. Natl. Bur. Stand. Sect. A 66 (1962) 13–28.
[22] J.D. Hoffman, Regime III crystallization in melt-crystallized polymers: the variable cluster model of chain folding, Polymer 24 (1983) 3–26.
[23] Y.T. Shieh, G.L. Liu, Y.K. Twu, T.L. Wang, C.H. Yang, Effects of carbon nanotubes on dynamic mechanical property, thermal property, and crystal structure of poly(L-lactic acid), J. Polym. Sci. Part B: Polym. Phys. 48 (2010) 145–152.
[24] L. Wen, Z. Xin, D. Hu, A new route of manipulation of poly(L-lactic acid) crystallization by self-assembly of p-tert-butylcalix[8] arene and toluene, J. Polym. Sci. Part B: Polym. Phys. 48 (2010) 1235–1243.
[25] M. Avrami, Kinetics of phase change. I general theory, J. Chem. Phys. 7 (1939) 1103–1112.
[26] M. Avrami, Kinetics of phase change. II transformation time relations for random distribution of nuclei, J. Chem. Phys. 8 (1940) 212–224.
[27] K.H. Illers, Polymorphism, crystallinity and melting enthalpy of poly(ε-caprolactam), 2. Calorimetric studies, Angew. Makromol. Chem. 179 (1978) 497–507.
[28] K.C. Yen, E.M. Woo, Thermodynamic and kinetic thermal analyses on dual crystal forms in polymorphic poly(heptamethylene terephthalate), J. Polym. Sci. Part B: Polym. Phys. 47 (2009) 1839–1851.
[29] Y. Yury, W.A. Paula, Rheological properties of crystallizing polylactide: detection of induction time and modeling the evolving structure and properties, J. Polym. Sci. Part B: Polym. Phys. 48 (2010) 812–822.
[30] K. Magniez, B.L. Fox, M.G. Looney, Nonisothermal crystallization behavior of poly(*m*-xylene adipamide)/montmorillonite nanocomposites, J. Polym. Sci. Part B: Polym. Phys. 47 (2009) 1300–1312.
[31] P. Cebe, S.D. Hong, Crystallization behaviour of poly(ether-ether-ketone), Polymer 27 (1986) 1183–1192.
[32] C.J. Tsai, M. Chen, H.Y. Lu, W.C. Chang, C.H. Chen, Crystal growth rates and master curves of poly(ethylene succinate) and its copolyesters using a nonisothermal method, J. Polym. Sci. Part B: Polym. Phys. 48 (2010) 932–939.
[33] G. Antoniadis, K.M. Paraskevopoulos, D. Bikiaris, K. Chrissafis, Melt-crystallization mechanism of poly(ethylene terephthalate)/multi-walled carbon nanotubes prepared by *in situ* polymerization, J. Polym. Sci. Part B: Polym. Phys. 47 (2009) 1452–1466.
[34] A.B. Felipe, Z.G. Ivan, R.D. Luisf, Z.G. Roberto, A.R. Sergio, Thermo-oxidative degradation of HDPE as a function of its crystalline content, J. Polym. Sci. Part B: Polym. Phys. 47 (2009) 1906–1915.
[35] J.D. Hoffman, G.T. Davis, J.I. Lauritzen, in: N.B. Hannay (Ed.), Treatise on Solid State Chemistry, Plenum Press, New York, 1976.
[36] S.F. Lu, M. Chen, Y.C. Shih, C.H. Chen, Nonisothermal crystallization kinetics of biodegradable poly(butylene succinate-co-propylene succinate), J. Polym. Sci. Part B: Polym. Phys. 48 (2010) 1299–1308.
[37] C.M. Wu, C.W. Jiang, Crystallization and morphology of polymerized cyclic butylene terephthalate, J. Polym. Sci. Part B: Polym. Phys. 48 (2010) 1127–1134.
[38] Y.T. Shieh, Y.K. Twu, C.C. Su, R.H. Lin, G.L. Liu, Crystallization kinetics study of poly(L-lactic acid)/carbon nanotubes nanocomposites, J. Polym. Sci. Part B: Polym. Phys. 48 (2010) 983–989.
[39] M.M. Favaro, B.T. Rego, M.C. Branciforti, R.E.S. Bretas, Study of the quiescent and shear-induced crystallization kinetics of intercalated PTT/MMT nanocomposites, J. Polym. Sci. Part B: Polym. Phys. 48 (2010) 113–127.
[40] H.S. Xu, X.J. Dai, P.R. Lamb, Z.M. Li, Poly(L-lactide) crystallization induced by multiwall carbon nanotubes at very low loading, J. Polym. Sci. Part B: Polym. Phys. 47 (2009) 2341–2352.
[41] M.L. Willians, R.F. Landel, J.D. Ferry, The temperature dependence of relaxation mechanisms in amorphous polymers and other glass-forming liquids, J. Am. Chem. Soc. 77 (1955) 3701–3707.
[42] Z.K. Zhong, Q.P. Guo, Crystallization kinetics of crosslinkable polymer complexes of novolac resin and poly(ethylene oxide), J. Polym. Sci. Part B: Polym. Phys. 37 (1999) 2726–2736.